Control Engineering Practice 16 (2008) 1329– 1343

Contents lists available at ScienceDirect

Control Engineering Practice

journal homepage: www.elsevier.com/locate/conengprac

Stability and performance in delayed bilateral teleoperation: Theory and experiments

A. Aziminejad [a,b,*], M. Tavakoli [c], R.V. Patel [a,b], M. Moallem [d]

[a] *Department of Electrical and Computer Engineering, University of Western Ontario, London, ON, Canada N6A 5B9*
[b] *Canadian Surgical Technologies and Advanced Robotics (CSTAR), 339 Windermere Road, London, ON, Canada N6A 5A5*
[c] *School of Engineering and Applied Sciences, Harvard University, 60 Oxford Street, Cambridge, MA 02138, USA*
[d] *The School of Engineering Science, Simon Frasier University, Surrey, BC V3T 0A3, Canada*

ARTICLE INFO

Article history:
Received 24 May 2007
Accepted 5 March 2008
Available online 7 May 2008

Keywords:
Bilateral teleoperation
Passivity
Transparency
Wave variables
Time delay

ABSTRACT

In the presence of communication latency in a bilaterally controlled teleoperation system, stability and transparency are severely affected. In this paper, based on a passivity framework, admittance-type and hybrid-type delay-compensated communication channels, which warrant different bilateral control architectures, are introduced. Wave transforms and signal filtering are used to make the delayed-communication channel passive and passivity/stability conditions are derived based on the end-to-end model of the teleoperation system with and without incorporating force measurement data of the master and the slave manipulators' interactions with the operator and the remote environment in the control configuration. Based on analogies of the hybrid parameters of the teleoperation systems, it is demonstrated that using force sensor measurements about hand/master and/or slave/environment interactions in the control algorithm can significantly improve teleoperation transparency. Experimental results with a soft-tissue task for a hybrid-type architecture and for round-trip delays of 60 and 600 ms further substantiate the hypothesis that using slave-side force measurements considerably enhances the matching of the master and the slave forces and consequently the transparency compared to a position error-based configuration.

1. Introduction

A teleoperation system enables human interaction with environments that are inaccessible to direct human contact due to their remoteness or the presence of hazards. Telesurgery and space telerobotics are two examples of more recent teleoperation applications involving long distance communication between master and slave units (Guthart & Salisbury, 2000; Butner & Ghodoussi, 2003; Sheridan, 1995). Recent interest in robot-assisted surgery is backed by advantages such as minimal invasiveness, enhanced accuracy and dexterity, and increased safety and reliability brought about by master/slave operations (Preusche, Ortmaier, & Hirzinger, 2002; Tavakoli, Patel, & Moallem, 2005). Telesurgery takes this one step further by its potentials for providing access to expert medical care for a larger group of patients more effectively and cost efficiently. Haptic feedback has been shown to improve task performance during both surgical and space teleoperation applications (Imaida, Yokokohji, Doi, Oda, & Yoshikawa, 2004; Wagner, Stylopoulos, & Howe, 2002).

From an engineering point of view, the main goals of teleoperation are twofold: stability and transparency. Transparency is the ability of a teleoperation system to present the undistorted dynamics of the remote environment to the human operator (Hannaford, 1989). The ability to do so is affected by the closed-loop dynamics of the master and the slave robots, which distort the dynamics of the remote environment as perceived by the human operator (Lawrence, 1993; Yokokohji & Yoshikawa, 1994). Among the more relevant aspects of teleoperation is an interesting control problem resulting from the presence of a non-negligible time delay in the communication media between the master and the slave. In the presence of time delays, the stability and transparency of a bilateral teleoperation system are severely affected. Several approaches have been proposed in the literature to deal with this problem. For a comprehensive overview and comparison on various time delay compensation methods, one can refer to Hokayem and Spong (2006), Arcara and Melchiorri (2002), Mascolo (2006), and Lin, Chen, and Huang (2008).

Scattering theory and its intuitively reformulated derivation, the wave transformation approach, are theoretically capable of

* Corresponding author at: Department of Electrical and Computer Engineering, University of Western Ontario, London, ON, Canada N6A 5B9.
E-mail addresses: aazimin@uwo.ca (A. Aziminejad), tavakoli@seas.harvard.edu (M. Tavakoli), rajni@eng.uwo.ca (R.V. Patel), mmoallem@sfu.ca (M. Moallem).

0967-0661/$ - see front matter © 2008 Elsevier Ltd. All rights reserved.
doi:10.1016/j.conengprac.2008.03.005

achieving stability independent of time delays (Anderson & Spong, 1989; Niemeyer & Slotine, 1991). Both of these approaches are based on passivity, which is a sufficient condition for stability (Desoer & Vidyasagar, 1975). The key objective for these approaches is to make the non-passive communication medium with time delay passive at the expense of transparency degradation. As will be further elaborated in Section 2.2 of this paper, based on different choices of wave transformation arrangements, the existing paradigm of a wave-based two-channel delay-compensated teleoperation system can be divided into two main sub-categories; admittance-type (symmetric) architecture and hybrid-type (asymmetric) architecture. In both cases, the teleoperation system stability and transparency are affected by the presence or absence of force sensing in the system. Specifically, it has been shown that transparency is improved in a delay-free teleoperation system when slave/environment force measurements are used (termed the kinesthetic force-based (KFB) approach in this paper (Aliaga, Rubio, & Sanchez, 2004; Sherman, Cavusoglu, & Tendick, 2000)). In this work, the question of stability of different wave-based two-channel teleoperation configurations is explicitly addressed and their performance in terms of transparency is comparatively evaluated. The main contributions of this paper are as follows:

- Stability of admittance-type teleoperation systems is investigated using a scattering matrix analysis approach of the end-to-end model of the teleoperation system (the master + communication channel + the slave) in Section 3. In particular, contrary to a commonly held view that using force sensors is not desirable due to its negative effect on stability, it is shown that stability can be maintained in the presence of force sensing and closed-form conditions for stable operation of different admittance-type configurations are derived. Wave-domain low pass filters are also factored into the analysis and it is demonstrated that they can be used as a design tool for adjusting the robust stability margin.
- Based on a single-loop modeling approach for the hybrid-type teleoperation system presented in Section 4, the stability of different hybrid-type configurations is examined. Specifically, it is demonstrated that using slave/environment force measurements does not necessarily render such a hybrid-type teleoperation system unstable. Unlike the admittance-type architecture, the absence of symmetry in the hybrid-type architecture makes the scattering matrix analysis method for analyzing stability mathematically intractable. To the best of the authors' knowledge, the above issues have not been addressed previously.
- Analytical and experimental transparency evaluations for different bilateral control configurations in Section 5 are indicative of significant improvements when force sensing is utilized during delayed teleoperation. Practical considerations suggest that it is more advantageous to use a hybrid-type configuration instead of an admittance-type one.

In Section 5, the theoretical work presented here is supported by experimental results based on a haptics-based teleoperation test-bed for minimally invasive surgery for two different values of round-trip time delays 60 and 600 ms, in order to address the effects of both moderate and large time delays.

2. Passivity and robust stability

Throughout the main part of this work, a single degree-of-freedom (DOF) linear teleoperation system is assumed with the following equations of motions for the master and the slave manipulators:[1]

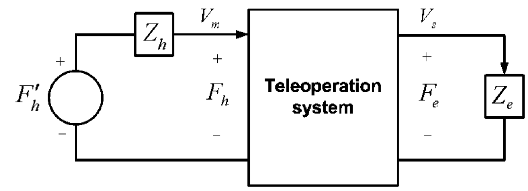

Fig. 1. Equivalent circuit representation of a teleoperation system.

$$M_m\ddot{x}_m = -f_m + f_h, \quad M_s\ddot{x}_s = f_s - f_e \tag{1}$$

where M_m and M_s are the master and slave inertias, f_m and f_s are the master and slave control actions, and x_m and x_s are the master and slave positions. Also, f_h and f_e represent the interaction forces between the operator's hand and the master, and the slave and the remote environment, respectively. In order to keep the mathematical analysis tractable, the nonlinear effects of friction and backlash have not been considered in the dynamic modeling of the bilateral teleoperation system. For an independent study of the cited issues, the interested reader is referred to Guesalaga (2004), Dodds and Glover (1995), and Mahvash and Okamura (2006).

Colgate (1993) has given the following intuitive condition for stability robustness: *A bilateral teleoperation system is said to be robustly stable if, when coupled to any passive environment, it presents to the operator an impedance (admittance) which is passive.* It is generally assumed that the human operator is passive, i.e., the operator does not do actions to make the system unstable. On the other hand, although the human operator can often help stabilize this system, this is a distraction from the task at hand, and more importantly, a violation of the assumption of operator passivity, and therefore not considered in stability analysis presented in this paper. By considering input and output velocities and forces in a teleoperation system as currents and voltages, an equivalent circuit representation of the system can be obtained (Fig. 1), in which impedances $Z_h(s)$, $Z_m(s) = M_m s$, $Z_s(s) = M_s s$, and $Z_e(s)$ denote dynamic characteristics of the human operator's arm, the master robot, the slave robot, and the remote environment, respectively, and f'_h is the exogenous input force from the operator. The equivalent two-port representation of a bilateral teleoperation system in Fig. 1 includes the master robot, the communication channel, and the slave robot. This equivalent circuit representation can be expressed by different two-port network models such as impedance, admittance, hybrid or scattering parameters. Not all multiport physical systems can be represented by impedance or admittance parameters, but for any LTI multiport system, a hybrid matrix exists and is defined as

$$\begin{bmatrix} F_h \\ -V_s \end{bmatrix} = \begin{bmatrix} h_{11} & h_{12} \\ h_{21} & h_{22} \end{bmatrix} \cdot \begin{bmatrix} V_m \\ F_e \end{bmatrix}. \tag{2}$$

2.1. Scattering theory and stability robustness

Based on its scattering matrix model, a teleoperation system is represented as $b = S(s)a$ where $a = [a_1 \quad a_2]^{\mathrm{T}}$ and $b = [b_1 \quad b_2]^{\mathrm{T}}$ are input and output waves of the teleoperation system, respectively. In a general two-port network, the relation between input and

[1] Here, it is assumed, without loss of generality, that the manipulator's dynamic model is decoupled and its parameters are fully known. A coupled manipulator with the dynamics $\underline{\tau} = \mathbf{M}\ddot{\underline{x}}$ where $\mathbf{M}$ has off-diagonal elements can be transformed to the decoupled system $\underline{\tau}' = \mathbf{N}\ddot{\underline{x}}$ using $\underline{\tau} = \mathbf{M}\mathbf{N}^{-1}\underline{\tau}'$ where $\mathbf{N}$ is a diagonal matrix of the same order as $\mathbf{M}$ (e.g., see Ahn & Yoon, 2002).

output waves and equivalent voltages and currents can be expressed as $a=(F+n^2V)/2$ and $b=(F-n^2V)/2$ where $F=[F_h \quad F_e]^{\mathrm{T}}$ and $V=[V_m \quad -V_s]^{\mathrm{T}}$ are the two-port's equivalent voltage and current vectors representing mechanical effort and flow pair force and velocity in the s domain, and n is a scaling factor. In a reciprocal network, $S_{12}=S_{21}$ and in a symmetric network $S_{11}=S_{22}$.

Theorem 1. *Necessary and sufficient conditions for robust stability of a teleoperation system are* (Colgate, 1993): (a) *$S(s)$ contains no poles in the closed right half plane* (*RHP*); *and* (b) *if Δ is the structured perturbation of S*

$$sup_{\omega}[\mu_{\Delta}(S(\mathrm{j}\omega))]\leqslant 1 \tag{3}$$

where $\mu_{\Delta}(S)$ is the structured singular value of matrix S.

A useful property for $\mu_{\Delta}(S)$ is (Colgate, 1993)

$$\mu_{\Delta}(S)\leqslant\bar{\sigma}(S) \tag{4}$$

where $\bar{\sigma}(\Delta)$ is the maximum singular value of Δ. The equality in (4) holds if the network is reciprocal (Yamamoto & Kimura, 1995). Theorem 1 enables us to use an *end-to-end* model of the teleoperation system for robust stability study based on the scattering matrix analysis. This removes any assumption on the passivity of the master + controller or the slave + controller blocks and only assumes that the operator and the environment are passive. This issue is further discussed in the next section.

2.2. Passivity-based time delay compensation

In the presence of a time delay, an ideally transparent bilateral teleoperation system has the following corresponding hybrid and scattering representation:

$$H=\begin{bmatrix} 0 & \mathrm{e}^{-sT} \\ -\mathrm{e}^{-sT} & 0 \end{bmatrix},\quad S=\begin{bmatrix} -\tanh(sT) & \mathrm{sech}(sT) \\ \mathrm{sech}(sT) & \tanh(sT) \end{bmatrix}. \tag{5}$$

It can be shown that $\bar{\sigma}(S)$ for this scattering matrix is unbounded; consequently this system cannot maintain robust stability. In practice, robust stability and transparency are competing issues in a teleoperation system (Lawrence, 1993). In other words, the smaller $\bar{\sigma}(S)$ is for a teleoperation system, the larger are the stability margin of the system and the stability robustness of the closed-loop system against variations in the dynamics parameters of the master, the slave, and the controller. Therefore, one can intuitively argue that $\bar{\sigma}(S)=1$ is the optimum choice for maintaining stability while the system operates with the best achievable transparency possible. A physical interpretation for a two-port network with $\bar{\sigma}(S)=1$ is the ideal transmission line with time delay, which can be represented by its corresponding hybrid and scattering models as

$$H=\begin{bmatrix} \tanh(sT) & \mathrm{sech}(sT) \\ -\mathrm{sech}(sT) & \tanh(sT) \end{bmatrix},\quad S=\begin{bmatrix} 0 & \mathrm{e}^{-sT} \\ \mathrm{e}^{-sT} & 0 \end{bmatrix}. \tag{6}$$

Comparing Eqs. (5) and (6), it can be seen that in the delayed transmission line robust stability has been attained at the expense of degraded transparency. Based on this argument, the following control law was proposed in Anderson and Spong (1989), which makes passive a communication channel with time delay in a

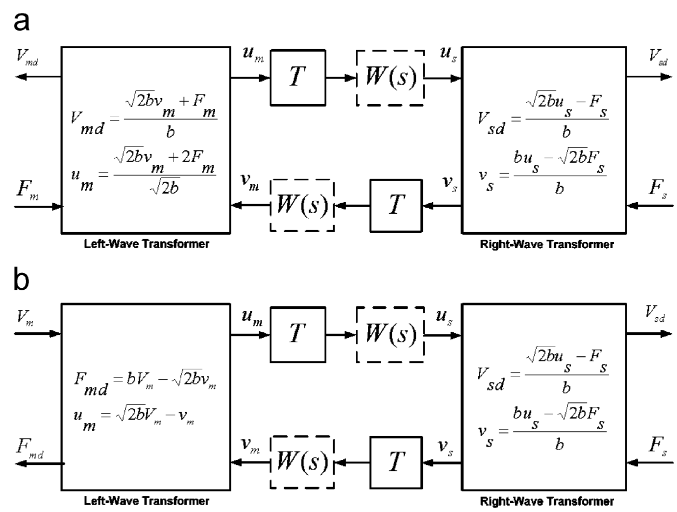

Fig. 2. (a) Admittance-type and (b) hybrid-type delay-compensated communication channels.

two-channel bilateral teleoperation system:

$$\begin{aligned} F_{md} &= F_s\,\mathrm{e}^{-sT}+n^2(V_m-V_{sd}\,\mathrm{e}^{-sT}),\\ V_{sd} &= V_m\,\mathrm{e}^{-sT}+n^{-2}(F_{md}\,\mathrm{e}^{-sT}-F_s). \end{aligned} \tag{7}$$

An energy-based approach, which yields the same results in a more physically motivated manner, was proposed in (Niemeyer & Slotine, 1991). A pair of wave variables (u,v) is defined based on a pair of standard power variables $(\dot{x},f)$ by the following:

$$u=\frac{b\dot{x}+f}{\sqrt{2b}},\quad v=\frac{b\dot{x}-f}{\sqrt{2b}} \tag{8}$$

where u denotes the right moving wave while v denotes the left moving wave. The characteristic wave impedance b is a positive constant and assumes the role of a tuning parameter. Eq. (8) are unique and invertible, meaning that they provide a transformation between power (any effort and flow pair) and wave variables. Using appropriate pairs of left and right wave transforms at the two ends of a non-passive communication channel with time delay can make it passive.

Depending on the choice of input/output pairs from the four variables in Eqs. (8), four two-port network models (architectures) are distinguished for the delay-compensated communication channel. These four architectures correspond to well-known representations of a two-port network as an impedance matrix, an admittance matrix, a hybrid matrix, or an inverse hybrid matrix. Among these four architectures, in order to operate the slave under velocity (position) control, the two cases in which the slave velocity is an output, namely the admittance-type (Fig. 2a) and the hybrid-type (Fig. 2b) delay-compensated channels, are of interest to us. In the equivalent two-port network of the admittance-type architecture, the transmitted master and slave velocities are outputs and the master and slave control actions (or forces) are inputs. Consequently, the equivalent electrical circuit representation of the system is symmetric. In the hybrid-type architecture, however, the slave velocity and the force transmitted to the master side are outputs, thus the corresponding equivalent circuit is asymmetric. In each architecture, based on the absence or presence of force sensing at the master and/or the slave sides, two control configurations are possible; namely position error-based (PEB) or kinesthetic force-based (KFB). In this paper, the time delay T has been assumed to be constant and equal in both directions.[2]

In the presence of time delay, the stability of wave-based admittance-type and hybrid-type PEB configurations has been studied using the traditional passivity framework (Niemeyer & Slotine, 1991). This approach is based on modeling the teleoperation system as a cascade of several two-port networks, among which only passivity of the delayed communication channel is ensured while passivity of the other blocks (human operator, master + controller, slave + controller, and environment) is assumed. The overall system passivity is based on the fact that the cascade interconnection of any two passive systems is passive. However, the cited approach cannot be applied to the case of a wave-based KFB teleoperation system as it cannot be modeled as a cascade of several two-port networks. As such, both Anderson and Spong (1989) and Niemeyer and Slotine (1991) have avoided the use of force sensor measurements due to questions which may arise about the passivity of the whole system. In this paper, the question of stability of admittance-type teleoperation systems is addressed using a less conservative approach, which is based on an *end-to-end* two-port model of the teleoperation system rather than the aforementioned cascade of two ports. Furthermore, a single-loop model of the entire teleoperation system (excluding the human operator and the environment) is presented to investigate the stability of hybrid-type teleoperation systems. As a result, in addition to proposing an approach to the stability analysis of KFB teleoperation systems under time delay, new robust stability conditions are provided for the PEB configurations under time delay. Moreover, the topic of transparency of wave-based admittance-type and hybrid-type architectures in the presence of time delay is subjected to a quantitative investigation.

In practice, a wave-based teleoperation system performance can be degraded due to a number of reasons, among which are discrete implementation of continuous-time control laws and significant variations in the operator's behavior or the environment impedance. The performance is particularly degraded for large time delays where high-frequency oscillations appear in the teleoperation system. Wave-domain low pass filtering can be used as a remedy for reducing vibrations and improving performance in the teleoperation system, specially when the impedance matching scheme of Niemeyer and Slotine (1991) and Tanner and Niemeyer (2006) fails to achieve the goal of performance improvement. In this paper, a wave-domain low pass filter $W(s)$ is also included in the stability analysis as shown in Fig. 2. The resulting stability conditions that are dependent on the bandwidth of $W(s)$ are particularly useful for maintaining a desired stability margin.

3. Admittance-type configurations

3.1. APEB and filtered APEB

An admittance-type position error-based (APEB) teleoperation system is illustrated in Fig. 3a. In this section, robust stability of the cited system is investigated based on an end-to-end model. Let us take $M_m = M_s = M$ and PD position controllers $C_m(s) = C_s(s) = (k_d s + k_p)/s$ used at the master and the slave. Also, let $W(s) = 1$ for now. The resulting teleoperation system has a

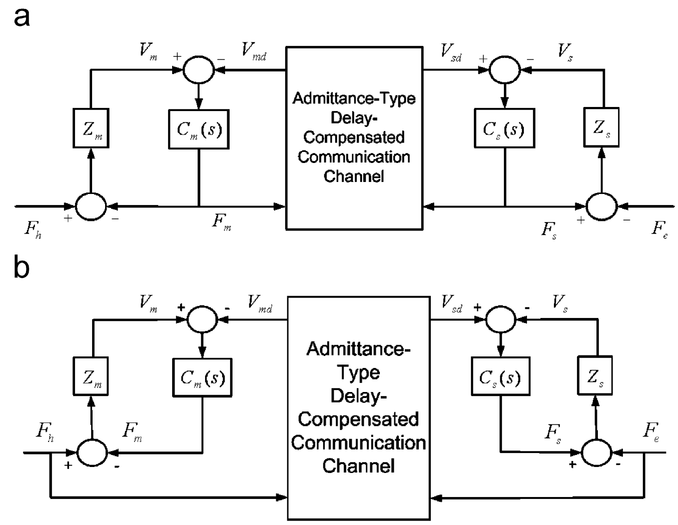

Fig. 3. Wave-based admittance-type teleoperation systems: (a) APEB; (b) AKFB.

scattering matrix that is both reciprocal and symmetric. As a result, investigating system stability using Theorem 1 is analytically tractable. In the neighborhood of $T = 0$ (fairly small time delays), by using a first-order Pade approximation for the exponential terms in the characteristic polynomial of the S matrix, it can be inferred that the sufficient condition for S to be RHP analytic is $k_d > 0$ and $k_p > 0$. Singular values of the scattering matrix of the APEB teleoperation system shown in Fig. 3a are

$$\sigma_{1,2}(s) = \left| \frac{(A_1 - B_1 + C_1 - D_1)e^{-sT} \pm (A_1 + B_1 - C_1 - D_1)}{(A_1 - B_1 - C_1 + D_1)e^{-sT} \pm (A_1 + B_1 + C_1 + D_1)} \right| \tag{9}$$

where $A_1 = Mbs^2 + bk_d s + bk_p$, $B_1 = Ms(k_d s + k_p)$, $C_1 = k_d s + k_p$, and $D_1 = bs$. According to condition (b) of Theorem 1, for the APEB teleoperation system to be passive and consequently robustly stable, $\sigma_{1,2}(j\omega) \leqslant 1$. Applying these conditions to (9) leads to

$$2b^2 k_d \omega^2 [1 \pm \cos(\omega T)] \geqslant 0 \tag{10}$$

As $k_d > 0$, both of the inequalities in (10) hold regardless of ω or T. In other words, according to (10) it can be concluded that the APEB teleoperation system is robustly stable as long as $k_d > 0$ and $k_p > 0$.

If a wave-domain low pass filter $W(s) = (Ls + 1)^{-1}$ is used in the APEB teleoperation system where $L = (2\pi f_{\text{cut}})^{-1}$ and f_{cut} is the cutoff frequency of the $W(s)$, the stability conditions will be (a) $k_d > 0$ and $k_p > 0$ as sufficient conditions, and (b) the singular values of the new scattering matrix will be the same as (9) if e^{-sT} is replaced by $e^{-sT}W(s)$. Applying the passivity condition to these new singular values gives (see Appendix A)

$$\frac{L^2[k_d \omega^2 (b + k_d) + k_p^2] + 2bk_d}{2bk_d \sqrt{1 + L^2}} \geqslant |\cos(\omega T + \varphi)| \tag{11}$$

where $\tan(\varphi) = L$. For $L = 0$, (11) simplifies to (10). Condition (11) defines a region of stability for a filtered APEB teleoperation system. A simplified region for robust stability can be determined if (11) is converted to

$$\frac{L^2[k_d \omega^2 (b + k_d) + k_p^2] + 2bk_d}{2bk_d \sqrt{1 + L^2}} \geqslant 1. \tag{12}$$

If rearranged and solved with respect to L, (12) imposes the following lower limit on L such that the filtered APEB teleopera-

[2] The assumption of equal forward and backward delay is not necessary for passivity of a wave-based delay-compensated communication channel and the only restriction which should be placed on the communication channel is that the delay remains constant. However, an assumption of different forward and reverse time delays does not have a significant effect on the derivations in this work and only adds to their mathematical complexity.

tion system is robustly stable

$$L_{\text{low}} = 2\frac{\sqrt{-k_p^2 bk_d + b^2k_d^2 - k_d^3\omega^2 b - k_d^2\omega^2 b^2}}{k_d\omega^2 b + k_d^2\omega^2 + k_p^2}. \tag{13}$$

A real L_{low} from (13), which necessitates $bk_d > k_p^2 + k_d\omega^2(k_d + b^2)$, corresponds to an upper limit for f_{cut}, which shows the cutoff frequency of the wave-domain low pass filter cannot become arbitrarily large. In other words, a lower cutoff frequency for the wave-domain filter ensures a better robust stability margin for the system. In the next section, it will be discussed that this higher stability margin comes at the expense of a lower level of transparency.

3.2. AKFB and filtered AKFB

In this section, a new symmetric two-channel wave-based teleoperation configuration is proposed which uses force sensing at both the master and the slave ends. The stability analysis reveals that stability can be maintained in this configuration and the corresponding robust stability conditions are derived.

Fig. 3b depicts a wave-based admittance-type kinesthetic force-based (AKFB) teleoperation configuration, in which measurements of hand/master and slave/environment interaction forces are used. With respect to stability, due to reciprocity and symmetry of its scattering matrix, an AKFB teleoperation system can be subjected to a scattering matrix analysis. Similar to the APEB configuration, a sufficient condition set for meeting criterion (a) of Theorem 1 is $k_d > 0$ and $k_p > 0$. For investigating criterion (b), singular values of the scattering matrix of the AKFB teleoperation system are derived as

$$\sigma_{1,2}(s) = \left|\frac{(A_2 + B_2 - C_2)\mathrm{e}^{-sT} \pm (A_2 - B_2 - C_2)}{(A_2 - B_2 + C_2)\mathrm{e}^{-sT} \pm (A_2 + B_2 + C_2)}\right| \tag{14}$$

where $A_2 = Mbs^2 + bk_d s + bk_p$, $B_2 = k_d s + k_p$, and $C_2 = bs$. Applying the passivity condition to these singular values gives the following stability condition (see Appendix A):

$$\frac{b}{\sqrt{b^2 + \omega^2 M^2}} \geqslant |\cos(\omega T - \varphi)| \tag{15}$$

where $\tan(\varphi) = \omega M/b$. In this configuration, the region of stability is more limited in comparison to APEB. However, robust stability can be achieved through proper selection of system parameters. Choosing the system's parameters such that $\omega M \ll b$ ensures criterion (15).

If the low pass filter $W(s)$ is made use of in AKFB, the singular values of the new scattering matrix can be obtained from (14) through replacing e^{-sT} with $\mathrm{e}^{-sT}W(s)$. In this way, the corresponding stability condition is (see Appendix A)

$$\frac{\omega^2 L^2(bk_d - Mk_p + k_d^2) + L^2k_p^2 + 2bk_d}{2k_d\sqrt{(1 + \omega^2 L^2)(b^2 + \omega^2 M^2)}} \geqslant |\cos(\omega T - \varphi)| \tag{16}$$

where $\tan(\varphi) = \omega(M - bL)/(M\omega^2 L + b)$. Similar to (15), (16) can also be satisfied through proper choice of the relevant parameters. Again, a simplified form of condition (16) can be written as

$$\frac{\omega^2 L^2(bk_d - Mk_p + k_d^2) + L^2k_p^2 + 2bk_d}{2k_d\sqrt{(1 + \omega^2 L^2)(b^2 + \omega^2 M^2)}} \geqslant 1 \tag{17}$$

Criterion (17), which is a sufficient condition for (16), can provide us with a simpler design condition to determine the lower bound of L required for robust stability of the teleoperation system.

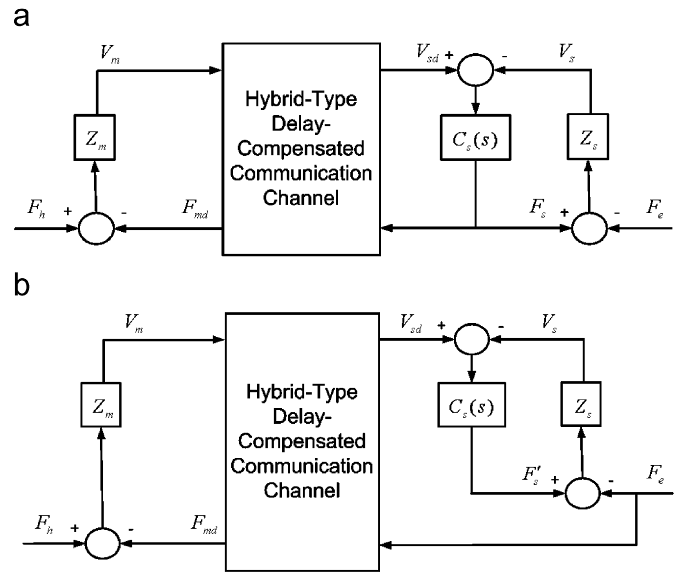

Fig. 4. Wave-based hybrid-type teleoperation systems: (a) HPEB; (b) HKFB.

4. Hybrid-type configurations

Fig. 4a shows a filtered HPEB configuration. In this section, a second hybrid-type teleoperation architecture is proposed (Fig. 4b), which utilizes slave/environment force measurement data (HKFB) and investigate the stability of both configurations.

In a hybrid-type teleoperation system, due to the asymmetric nature of the topology of the teleoperation architecture, the scattering matrix $S(s)$ is asymmetric and the eigenvalues of $S(s)$ are extremely involved making it very difficult to extract closed-form robust stability conditions. The bottomline is that, unlike the admittance-type (symmetric) architecture, stability study of a hybrid-type system through scattering matrix analysis is mathematically untractable. Alternatively, in order to conduct a stability analysis for both filtered HPEB and HKFB configurations, the teleoperation system is converted into a single-loop representation and the passivity theorem (Khalil, 2002) is utilized, as in the following.

4.1. Filtered HPEB

The hybrid-type delay-compensated communication channel in Fig. 4, which is shown in Fig. 2b, can be represented as

$$\begin{bmatrix} F_{md} \\ -V_{sd} \end{bmatrix} = H_{\text{ch}} \cdot \begin{bmatrix} V_m \\ F_s \end{bmatrix} \tag{18}$$

where H_{ch} is the hybrid model of the delay-compensated communication channel. Using Fig. 2b (including the wave-domain low pass filter $W(s)$) and (18), the entries of H_{ch} can be derived as

$$\begin{aligned} h_{11_{\text{ch}}} &= \frac{b[1 - \mathrm{e}^{-2sT}W(s)^2]}{\mathrm{e}^{-2sT}W(s)^2 + 1}, \\ h_{12_{\text{ch}}} &= \frac{2\,\mathrm{e}^{-sT}W(s)}{\mathrm{e}^{-2sT}W(s)^2 + 1} \\ h_{21_{\text{ch}}} &= -\frac{2\,\mathrm{e}^{-sT}W(s)}{\mathrm{e}^{-2sT}W(s)^2 + 1}, \\ h_{22_{\text{ch}}} &= \frac{1 - \mathrm{e}^{-2sT}W(s)^2}{b[\mathrm{e}^{-2sT}W(s)^2 + 1]}. \end{aligned} \tag{19}$$

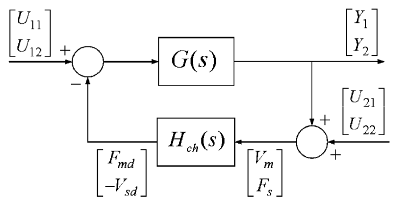

Fig. 5. Simplified single-loop feedback connection of a wave-based hybrid-type teleoperation system.

In order to apply the passivity theorem, Eqs. (1) and (18) along with $F_s = C_s(V_{sd} - V_s)$ can be rearranged in the form of the single-loop feedback system of Fig. 5 where H_{ch} is defined in (19) and

$$G = \begin{bmatrix} \frac{1}{Z_m} & 0 \\ 0 & \frac{C_s Z_s}{C_s + Z_s} \end{bmatrix}. \tag{20}$$

This single-loop representation includes the delay-compensated communication channel of Fig. 2b in its feedback path H_{ch} and the combination of the master, the slave, and the bilateral controller (Fig. 4a) in its feed-forward path G. For this single-loop representation, the inputs shown in Fig. 5 are $U_{11} = F_h$, $U_{12} = 0$, $U_{21} = 0$, $U_{22} = C_s F_e/(C_s + Z_s)$ and the outputs are $Y_1 = V_m$ and $Y_2 = V_{sd} C_s Z_s/(C_s + Z_s)$.

According to the passivity theorem, the conditions for the closed-loop map from input to output to be finite-gain $\mathscr{L}_2$ stable (i.e., all the signals remain bounded; for an LTI system, $\mathscr{L}_2$ stability implies BIBO stability) are passivity of G and strict passivity of H_{ch}. The strict passivity of H_{ch} can be checked by using Theorem 1. The corresponding scattering matrix entries for H_{ch} are

$$\begin{aligned} s_{11_{\text{ch}}} = s_{22_{\text{ch}}} &= \frac{(b^2 - 1)[W^2(s)\,\mathrm{e}^{-2sT} - 1]}{(b-1)^2 W^2(s)\,\mathrm{e}^{-2sT} - (b+1)^2} \\ s_{12_{\text{ch}}} = s_{21_{\text{ch}}} &= \frac{-4W(s) b\,\mathrm{e}^{-sT}}{(b-1)^2 W^2(s)\,\mathrm{e}^{-2sT} - (b+1)^2} \end{aligned} \tag{21}$$

The singular values for this scattering matrix are given as

$$\sigma_{1,2}(s) = \left| \frac{(b+1)W(s)\mathrm{e}^{-sT} \pm (b-1)}{(b-1)W(s)\mathrm{e}^{-sT} \pm (b+1)} \right| \tag{22}$$

Taking $s = \mathrm{j}\omega$, the passivity condition $\sigma_1, \sigma_2 \leqslant 1$, leads to

$$\frac{bL^2\omega^2}{1 + L^2\omega^2} \geqslant 0 \tag{23}$$

which is guaranteed if $b > 0$. According to (23), the margin for strict passivity of the delay-compensated channel is b as $L \to \infty$. However, excessive increase of L (or equivalently, reduction of f_{cut}) incurs a penalty on system transparency. On the contrary, $L \to 0$ results in marginal strict passivity of H_{ch} while improving transparency.

The condition of passivity for G is equivalent to G being a positive real matrix. Since G has a proper rational form and a nonzero determinant, it is positive real if $G(s)$ is Hurwitz, $G(\mathrm{j}\omega) + G^{\mathrm{T}}(-\mathrm{j}\omega)$ is positive semidefinite, and any pure imaginary pole $\mathrm{j}\omega$ of any element of $G(s)$ is a simple pole and the residue matrix $\lim_{s \to \mathrm{j}\omega}(s - \mathrm{j}\omega)G(s)$ is positive semidefinite Hermitian. It is straightforward to show that $G(s)$ in (20) possesses all the conditions for being positive real if $k_d > 0$ and $k_p > 0$. Note that the second output in the single-loop representation of the HPEB teleoperation system in Fig. 5 is proportional to V_{sd}, whereas the actual outputs of the system are V_m and V_s. This change of output does not pose a problem to the input–output finite gain $\mathscr{L}_2$ stability of the teleoperation system since with respect to F_e and V_{sd}, V_s can be written as

$$V_s = \frac{C_s V_{sd} - F_e}{Z_s + C_s}. \tag{24}$$

Since both F_e and V_{sd} are bounded signals (V_{sd} is the output of a finite gain $\mathscr{L}_2$ stable system) and the denominator in (24) is a Hurwitz polynomial, V_s also remains bounded. Moreover, in the presence of a passive remote environment modeled as $Z_e = F_e/V_s$, (24) can be rewritten as $V_s = C_s V_{sd}/(Z_s + C_s + Z_e)$. Assuming a mass–damper–spring model for the passive impedance Z_e, it can be deduced that V_s is still bounded (all the coefficients of the second-order characteristic polynomial remain nonnegative).

4.2. Filtered HKFB

For an HKFB teleoperation system, still using the delay-compensated communication channel of Fig. 2b, based on Fig. 4b and the single-loop equivalent representation of Fig. 5, matrix G has the following form:

$$G = \begin{bmatrix} \frac{1}{Z_m} & 0 \\ 0 & 0 \end{bmatrix} \tag{25}$$

The inputs of the single-loop representation are $U_{11} = F_h$, $U_{12} = 0$, $U_{21} = 0$, $U_{22} = F_e$ and the outputs are $Y_1 = V_m$ and $Y_2 = 0$. Similar to the case of the HPEB teleoperation system, for this single-loop representation to be input–output finite gain $\mathscr{L}_2$ stable, G has to be passive and H_{ch} has to be strictly passive. The communication channel is again given by (18) and (19), thus the strict passivity of H_{ch} has already been proven.

With respect to passivity of G, some analytical endeavor confirms that (25) meets all the conditions for being positive real. On the other hand, an actual output of the system, V_s, is related to bounded signals F_e and V_{sd} through Eq. (24). In order to have a bounded V_s, Eq. (24) should be RHP analytic. Therefore, a sufficient condition for input–output stability of the overall system is $k_d > 0$ and $k_p > 0$.

It is worth mentioning that the HPEB system has a reciprocal scattering matrix, thus passivity is the necessary and sufficient condition for robust stability. However, the HKFB system possesses a scattering matrix, which is neither symmetric nor reciprocal implying that, although sufficient, passivity is not a necessary condition for its robust stability. The interest in passivity of a teleoperation system stems from the fact that it ensures robustly stable performance for a class of multi-variable systems that cannot be easily subjected to other methods of stability analysis. Lastly, as was mentioned earlier in this section, a large value of L produces a larger margin for robust stability of the teleoperation but at the same time deteriorates teleoperation transparency.

5. Performance evaluation

For experimental evaluation, a force-reflective master/slave system developed as an endoscopic surgery test-bed (Fig. 6) has been used. Through the master interface, a user controls the motion of the slave arm and receives force/torque feedback of the slave/environment interactions. The master is capable of providing the user with force sensation and kinesthetic sensation of the elasticity of an object in all DOFs available in endoscopic surgery (pitch, yaw, roll, insertion, and handle open/close)—see Tavakoli, Patel, and Moallem (2006) for a detailed description of the haptic master interface. The developed slave arm is an endoscopic instrument capable of actuating the open/close motions of a tip

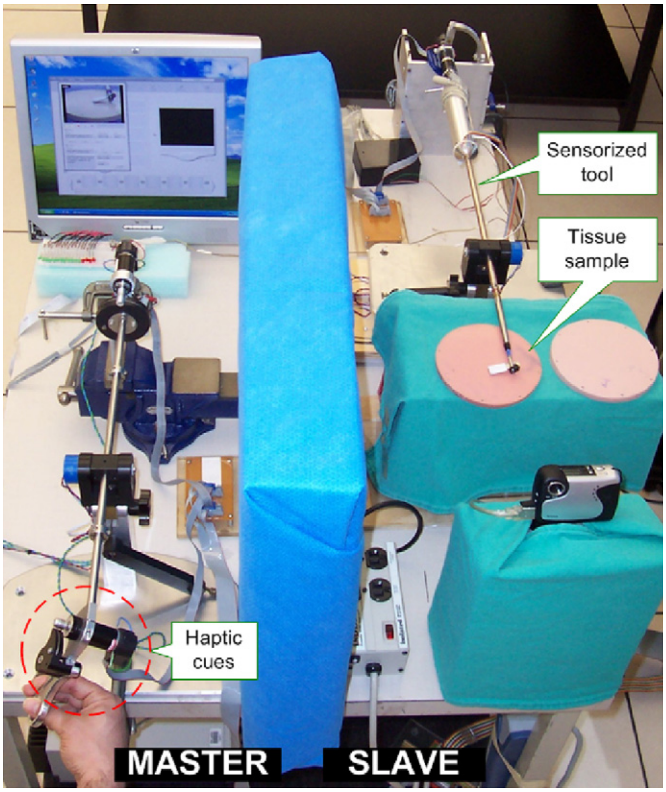

Fig. 6. Setup for telemanipulated tissue palpation.

and rotations about its main axis. Due to the problems posed by the incision size constraint in minimally invasive surgery, strain gauge sensors are integrated into the end effector to provide a non-invasive way of measuring interactions with tissue in all the five DOFs. For more information about the slave, see Tavakoli et al. (2005). In the experiments, the master and slave subsystems were constrained for force-reflective teleoperation in the twist direction only (i.e., rotations about the instrument axis). The instrument interactions with the tissue are measured and reflected in real-time to the user. The Virtual Reality Peripheral Network (www.vrpn.org) has been used for network-based communication such that the slave can be telemanipulated from the master. The digital control loop is implemented at a sampling frequency of 1000 Hz and circular buffers have been used to create adjustable time delays in the communication channel.

As discussed in Appendix B, the haptic master interface, the friction/gravity effects are determined and compensated for such that the user does not feel any weight on his/her hand when the slave is not in contact with an object. This master/slave system is a useful test-bed for investigating the performance and effectiveness of different tool/tissue interaction feedback modalities in soft-tissue applications. Appendix B also includes the master and the slave systems modelling and identification, whereby the friction-compensated master is represented as $\tau_m = M_m\ddot{\theta}_m$ and the slave's model is identified as $\tau_s = M_s\ddot{\theta}_s$.

5.1. Admittance-type configurations

In order to quantitatively evaluate transparency of a teleoperation system, its hybrid parameters can be utilized. Solving the equivalent two-port network's equations for F_h and $-V_s$ with respect to V_m and F_e for the teleoperation system in Fig. 3b, hybrid parameters of the AKFB configuration are derived as

$$\begin{aligned} h_{11} &= \frac{b(1-W^2\mathrm{e}^{-2sT})(Ms^2+sk_d+k_p)}{\Delta_1} \\ h_{12} &= -h_{21} = \frac{2(k_ds+k_p)W\,\mathrm{e}^{-sT}}{\Delta_1} \\ h_{22} &= \{(1-W^2\,\mathrm{e}^{-2sT})[(k_d^2+b^2)s^2+2k_pk_ds+kp^2] \\ &\quad +2bs(1+W^2\,\mathrm{e}^{-2sT})(k_ds+k_p)]\}/\Delta_2 \end{aligned} \tag{26}$$

where

$$\begin{aligned} \Delta_1 &= (k_ds+k_p)(1+W^2\,\mathrm{e}^{-2sT})+sb(1-W^2\,\mathrm{e}^{-2sT}) \\ \Delta_2 &= b(Ms^2+sk_d+k_p)\Delta_1. \end{aligned} \tag{27}$$

The hybrid parameter $h_{11} = F_h/V_m|_{F_e=0}$ is the input impedance in free-motion condition. The parameter $h_{12} = F_h/F_e|_{V_m=0}$ is a measure of force tracking for the haptic teleoperation system. The parameter $h_{21} = -V_s/V_m|_{F_e=0}$ is a measure of the velocity (or equivalently, position) tracking performance. Finally, $h_{22} = -V_s/F_e|_{V_m=0}$ is the output admittance when the master is motionless. When $T \to 0$ and $W(s) = 1$, the hybrid parameters in the AKFB teleoperation configuration can be approximated by

$$\begin{aligned} h_{11} &= 0, \quad h_{12} = -h_{21} = 1 \\ h_{22} &= \frac{2s}{Ms^2+sk_d+k_p}. \end{aligned} \tag{28}$$

Comparison of (28) with the hybrid matrix of an ideally transparent delayed teleoperation system represented by (5) when $T \to 0$ reveals that in this case the only non-ideal hybrid parameter is h_{22}.

For an APEB teleoperation system (Fig. 3a) the hybrid parameters are more complex in comparison to AKFB. However, in the similar situation of infinitesimal delays and $W(s) = 1$, they simplify to

$$\begin{aligned} h_{11} &= \frac{2Ms(Ms^2+sk_d+k_p)}{2Ms^2+sk_d+k_p} \\ h_{12} &= -h_{21} = \frac{k_ds+k_p}{2Ms^2+sk_d+k_p}, \\ h_{22} &= \frac{2s}{2Ms^2+sk_d+k_p}. \end{aligned} \tag{29}$$

By comparing (28) and (29) with the hybrid matrix of an ideally transparent teleoperation system when $T \to 0$, one can conclude that AKFB has a superior transparency over APEB.

The H-parameters versus human operator's input frequency for two typical APEB and AKFB teleoperation systems with identical parameters have been compared in Fig. 7 for a non-negligible amount of time delay. It has been assumed that $b = 1$, $T = 0.03$ s, $M_m = M_s = 0.1$ kg, $k_p = 100$, $k_d = 10$, and $f_{cut} = 10$ Hz. These figures support the conclusion about the superior transparency of AKFB in comparison to APEB. In order to further quantify the improvement in transparency gained through using the AKFB configuration in comparison to the APEB configuration in Fig. 7, the Integral of Absolute Error (IAE) has been calculated for deviations of the magnitudes of the hybrid parameters from their ideal values (zero for h_{11} and h_{22} and one for h_{12} and h_{21}) when the input frequency changes from 0 to 10 Hz (Table 1). In the case of AKFB configuration, the corresponding values of IAE in Table 1 represent 35%, 72%, and 72% improvement with respect to h_{11}, h_{12}, and h_{21}, respectively, and a 45% deterioration for h_{22}. It is worth mentioning that h_{22} is not as critical as the rest of hybrid parameters in providing a satisfactory level of transparency for the human operator since it basically represents the perception reflected to the remote environment by the teleoperation system.

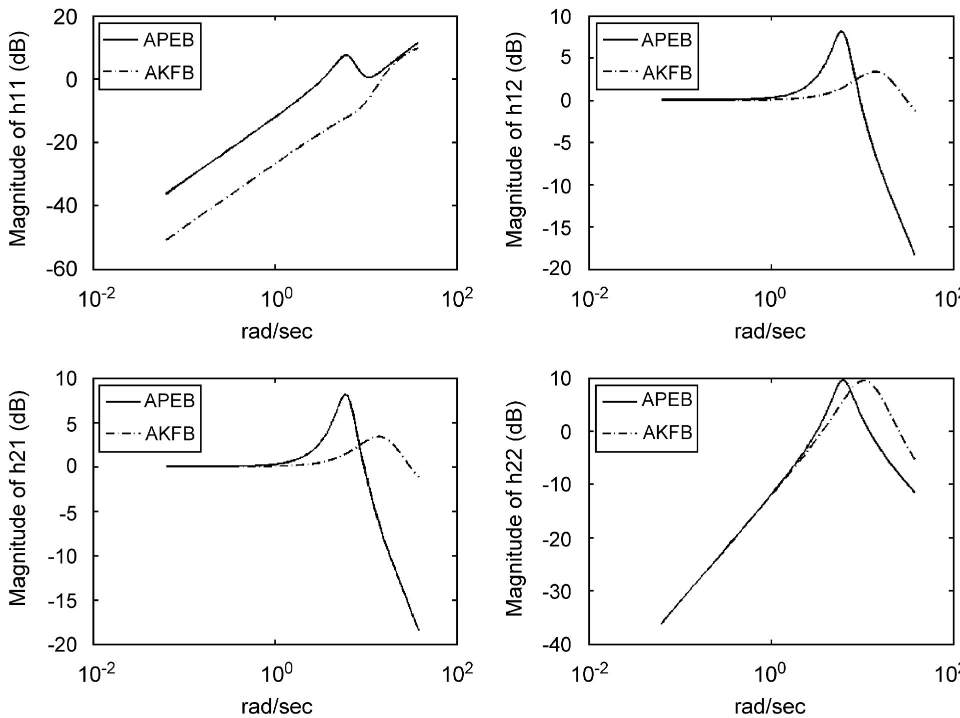

Fig. 7. Hybrid parameters for two typical APEB and AKFB teleoperation systems.

Table 1
IAE values for deviations of the magnitudes of the H-parameters of APEB and AKFB systems from their ideally transparent values

	APEB	AKFB
h_{11}	32.22	21.02
h_{12}	7.72	2.21
h_{21}	7.72	2.21
h_{22}	5.54	10.11

5.1.1. Implementation issues

The hybrid-type teleoperation configurations are particularly of interest because of an implementation advantage of hybrid-type configurations over admittance-type configurations. From the controller tuning point of view, assuming an APEB teleoperation system without time delay the closed-loop control law at the slave side is

$$sX_s = \frac{C_s E - F_e + M_s s^2 X_m}{Z_s} \tag{30}$$

where $E = X_m - X_s$ and $C_s = k_{ds}s + k_{ps}$. The acceleration feedback term $M_s s^2 X_m$ in (30) is necessary for asymptotic stability of the slave's closed-loop system. Eq. (30) can be rewritten as

$$M_s s^2 E + C_s E = F_e. \tag{31}$$

Similarly, at the master side

$$M_m s^2 E + C_m E = F_h. \tag{32}$$

Subtracting (31) from (32)

$$(M_m - M_s)s^2 E + (C_m - C_s)E = F_h - F_e. \tag{33}$$

In the ideal case $F_h = F_e$, hence

$$s^2 E + \frac{C_m - C_s}{M_m - M_s} E = 0. \tag{34}$$

Taking $(C_m - C_s)/(M_m - M_s) = C$ to be a PD controller ensures asymptotic convergence of $e(t)$ to zero. To this end, the master and the slave position controllers are chosen to be PD-type as $C_m = M_m C$ and $C_s = M_s C$, resulting in

$$\frac{C_m}{M_m} = \frac{C_s}{M_s}. \tag{35}$$

As the master and slave side parameters are not generally the same, neither APEB nor AKFB configurations have symmetric scattering matrices and therefore they cannot be subjected to an analytic stability study based on scattering matrix analysis. Alternatively, criterion (b) of Theorem 1 can be tested numerically versus the input frequency for a particular system with given parameters. As a practical example, assume $k_{ds} = 1$, $k_{ps} = 5$, $T = 100\,\text{ms}$, $b = 1$, and $f_{\text{cut}} = 10\,\text{Hz}$ in the experimental setup. Fig. 8 shows the numerical values of $\bar{\sigma}(S)$ for filtered APEB and filtered AKFB teleoperation schemes implemented on the setup versus the input frequency. The values of $\bar{\sigma}(S)$ for both systems remain less than 1 for the frequency range of interest, so both systems are robustly stable.

Based on (35), the slave-side PD controller is tuned for tracking under the free-motion condition, and the master-side controller will be a scaled version of that. The ultimate goal of tuning in a bilateral teleoperation system is to make the slave controller as "stiff" (i.e., highly accurate position control) as possible, while keeping the master as "compliant" (i.e., highly responsive to force control) as possible. However, by making the slave controller stiff through increasing its gains, according to (35), the outputs of the master and the slave controllers can saturate causing high-frequency vibrations in the system. On the other hand, excessive reduction of the slave controller gains will cause underdamped (and low-frequency oscillatory) response. In order to exemplify the nature of this problem, Fig. 9 shows the root locus plot of the dominant poles of the filtered APEB configuration implemented on the experimental setup for different values of the slave controller gain k_{ps}, when the slave is in free-motion condition

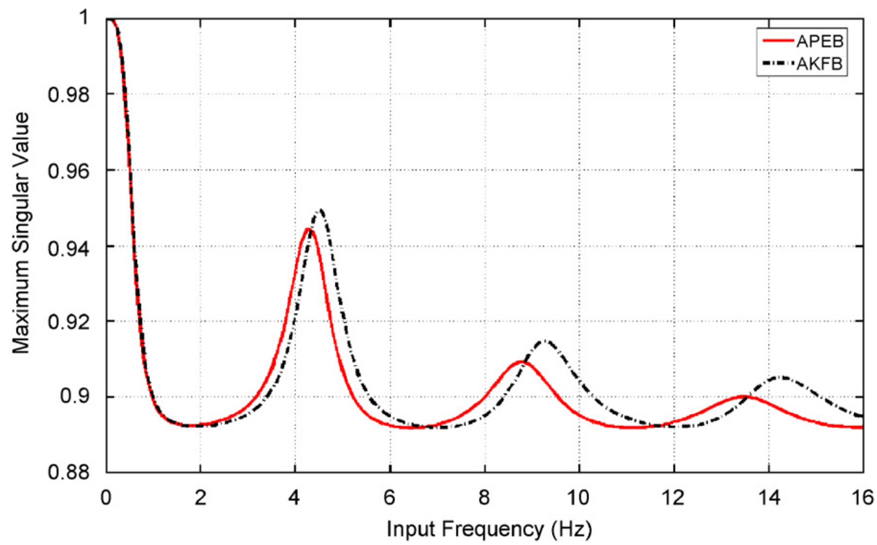

Fig. 8. Maximum singular value versus input frequency for filtered APEB and filtered AKFB.

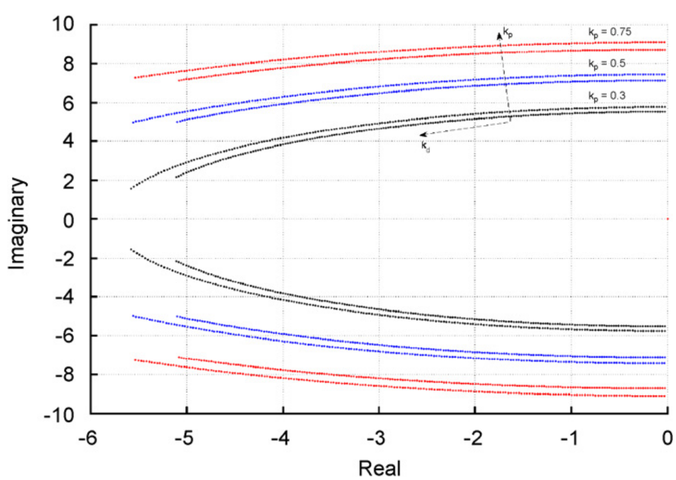

Fig. 9. Root loci of the dominant poles of a non-uniform filtered APEB architecture versus k_{ds} and k_{ps}.

($Z_e = 0$) and $0 < k_{ds} \leqslant 0.1$. For each choice of k_{ps}, the four loci of dominant poles start from pure imaginary values, and with increasing k_{ds}, move toward the points of entry on the real axis. As can be seen in Fig. 9, the range of the slave controller's gains for which saturation of the master and the slave controllers are avoided corresponds to a dominant pole location that leads to a very compliant and underdamped slave. In the presence of a nonzero Z_e, this situation further deteriorates since there is a pair of pure imaginary poles very close to the imaginary axis. The same principle is applicable to a filtered AKFB teleoperation system, which possesses half the number of dominant poles of a filtered APEB system. Fig. 10 shows two free-motion position tracking profiles of the APEB and AKFB systems, which have been acquired from the experimental setup. These profiles correspond to $T = 30\,\text{ms}$, $b = 1$, and $f_{\text{cut}} = 5\,\text{Hz}$. The values of k_{ps} and k_{ds} have been tuned for achieving optimum free-motion tracking, i.e., to achieve the stiffest slave while avoiding controllers saturation. It can be seen that in the experimental setup these optimum gains fall short of achieving perfect position tracking at the slave end, thus providing the practical motivation for using a hybrid-type teleoperation architecture.

5.2. Hybrid-type configurations

Using Fig. 4a and definition (2), the hybrid parameters for a filtered HPEB teleoperation system are derived as

$$\begin{aligned}
h_{11} &= \{(1 + W^2 e^{-2sT})sb[M_m M_s s^2 + k_d(M_m + M_s)s \\
&\quad + k_p(M_m + M_s)] + (1 - W^2 e^{-2sT})[k_d M_m M_s s^3 \\
&\quad + M_s(M_m k_p + b^2)s^2 + k_d b^2 s + k_p b^2]\}/\Delta_3 \\
h_{12} &= -h_{21} = 2bW e^{-sT}(sk_d + k_p)/\Delta_3 \\
h_{22} &= [(1 + W^2 e^{-2sT})sb + (1 - W^2 e^{-2sT})(sk_d + k_p)]/\Delta_3 \\
\Delta_3 &= (1 + W^2 e^{-2sT})b(M_s s^2 + k_d s + k_p) \\
&\quad + (1 - W^2 e^{-2sT})M_s s(k_d s + k_p)
\end{aligned} \tag{36}$$

and based on Fig. 4b for a filtered HKFB teleoperation system

$$\begin{aligned}
h_{11} &= \frac{(1 + W^2 e^{-2sT})M_m s + (1 - W^2 e^{-2sT})b}{(1 + W^2 e^{-2sT})} \\
h_{12} &= \frac{2W e^{-sT}}{(1 + W^2 e^{-2sT})} \\
h_{21} &= \frac{-2W e^{-sT}(sk_d + k_p)}{(1 + W^2 e^{-2sT})(M_s s^2 + k_d s + k_p)} \\
h_{22} &= \frac{(1 + W^2 e^{-2sT})sb + (1 - W^2 e^{-2sT})(sk_d + k_p)}{b(1 + W^2 e^{-2sT})(M_s s^2 + k_d s + k_p)}.
\end{aligned} \tag{37}$$

In order to have a better sense of the difference between these two configurations in terms of transparency, their hybrid parameters are compared for infinitesimal T and $W(s) = 1$. In this case, hybrid parameters of the HPEB configuration are simplified to

$$\begin{aligned}
h_{11} &= M_m s + \frac{M_s s(sk_d + k_p)}{M_s s^2 + k_d s + k_p} \\
h_{12} &= -h_{21} = \frac{sk_d + k_p}{M_s s^2 + k_d s + k_p}, \\
h_{22} &= \frac{s}{M_s s^2 + k_d s + k_p}
\end{aligned} \tag{38}$$

and for the case of the HKFB configuration

$$\begin{aligned}
h_{11} &= M_m s, \quad h_{12} = 1 \\
h_{21} &= -\frac{sk_d + k_p}{M_s s^2 + k_d s + k_p}, \\
h_{22} &= \frac{s}{M_s s^2 + k_d s + k_p}.
\end{aligned} \tag{39}$$

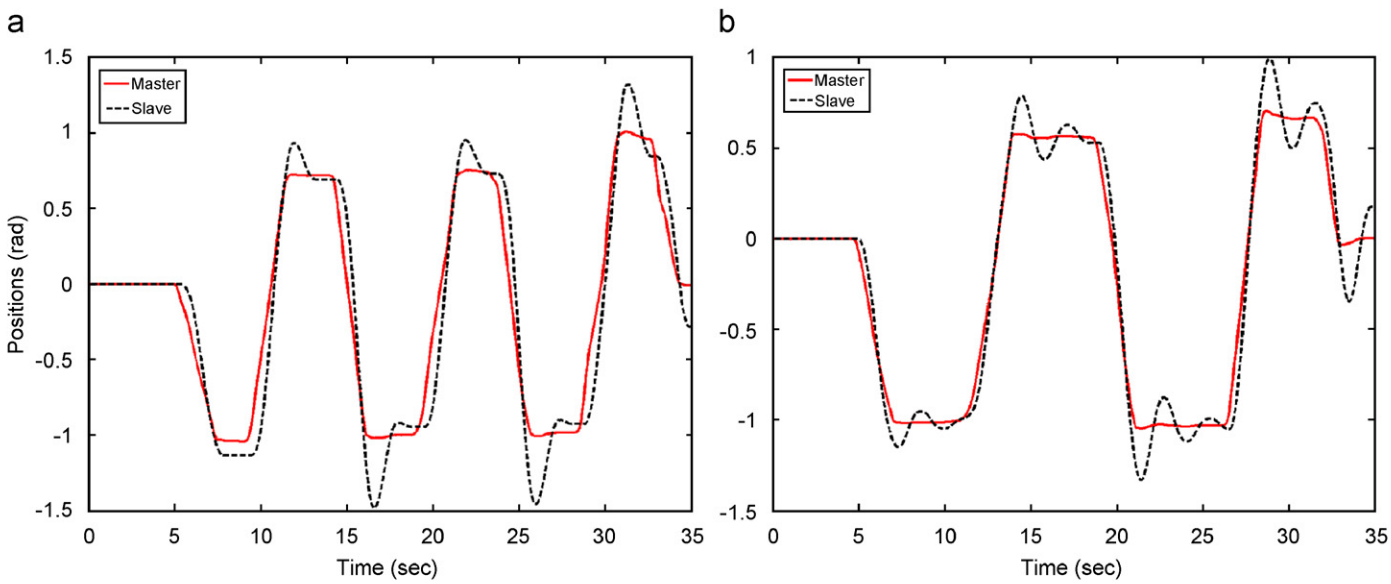

Fig. 10. Free-motion position tracking profiles for (a) APEB and (b) AKFB teleoperation systems with one-way delay $T = 30$ ms.

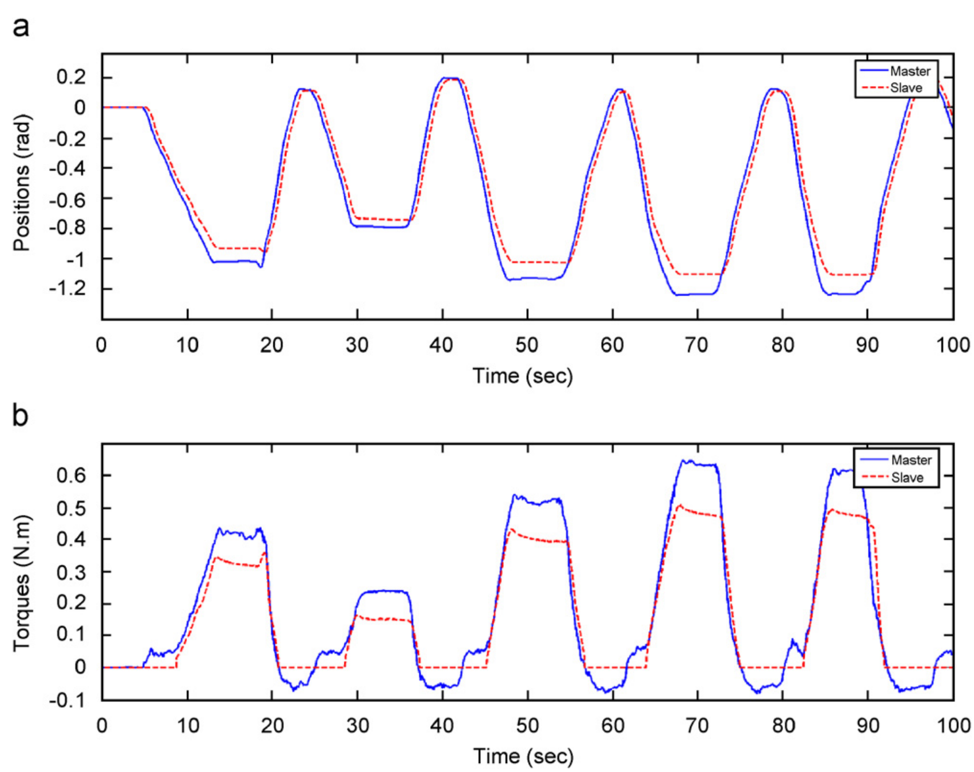

Fig. 11. (a) Position and (b) force tracking profiles for the HPEB teleoperation system with one-way delay $T = 30$ ms.

The value of h_{11} indicates that under HKFB control, a user only feels the master's inertia, which for a haptic device is fairly small, when the slave is performing a free-motion movement while the user receives a "sticky" feel of free-space motions under HPEB control. Moreover, the value of h_{12} in (39) is evidence of perfect force tracking in the HKFB teleoperation system. Consequently, by comparing (38) and (39) it is reasonable to say that the HKFB configuration performs more transparently than HPEB in terms of h_{11} and h_{12} and their performance is identical with respect to h_{21} and h_{22}.

In order to further substantiate the theoretical developments derived in this work, tissue palpation experiments were conducted with the experimental setup. For performing a soft-tissue palpation task (which is also utilized as a medical diagnostic procedure), the user manipulates the master causing the slave to probe the tissue via a small rigid beam attached to the endoscopic instrument. The user moves the master back and forth for 100 s. The slave interactions with the soft environment are reflected to the user via the master interface. For the palpation tests, an object made of packaging foam material was used. As mentioned earlier, the gravity effects in the master interface have been compensated for such that the user does not feel any weight when the slave's tip is not in contact with the object.

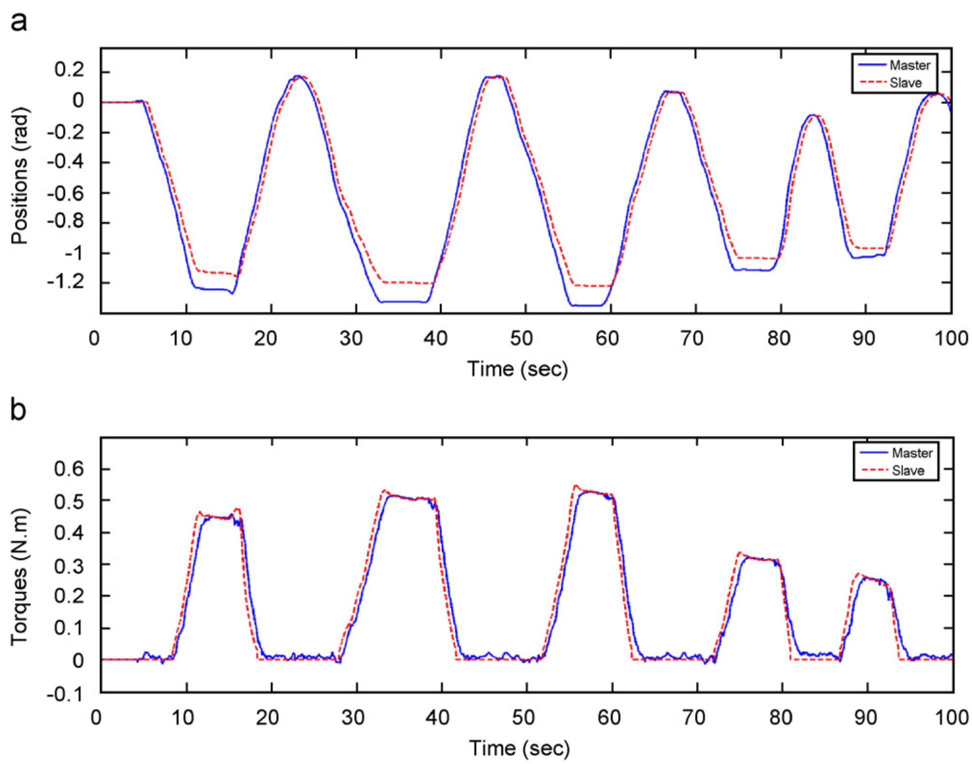

Fig. 12. (a) Position and (b) force tracking profiles for the HKFB teleoperation system with one-way delay $T = 30\,\text{ms}$.

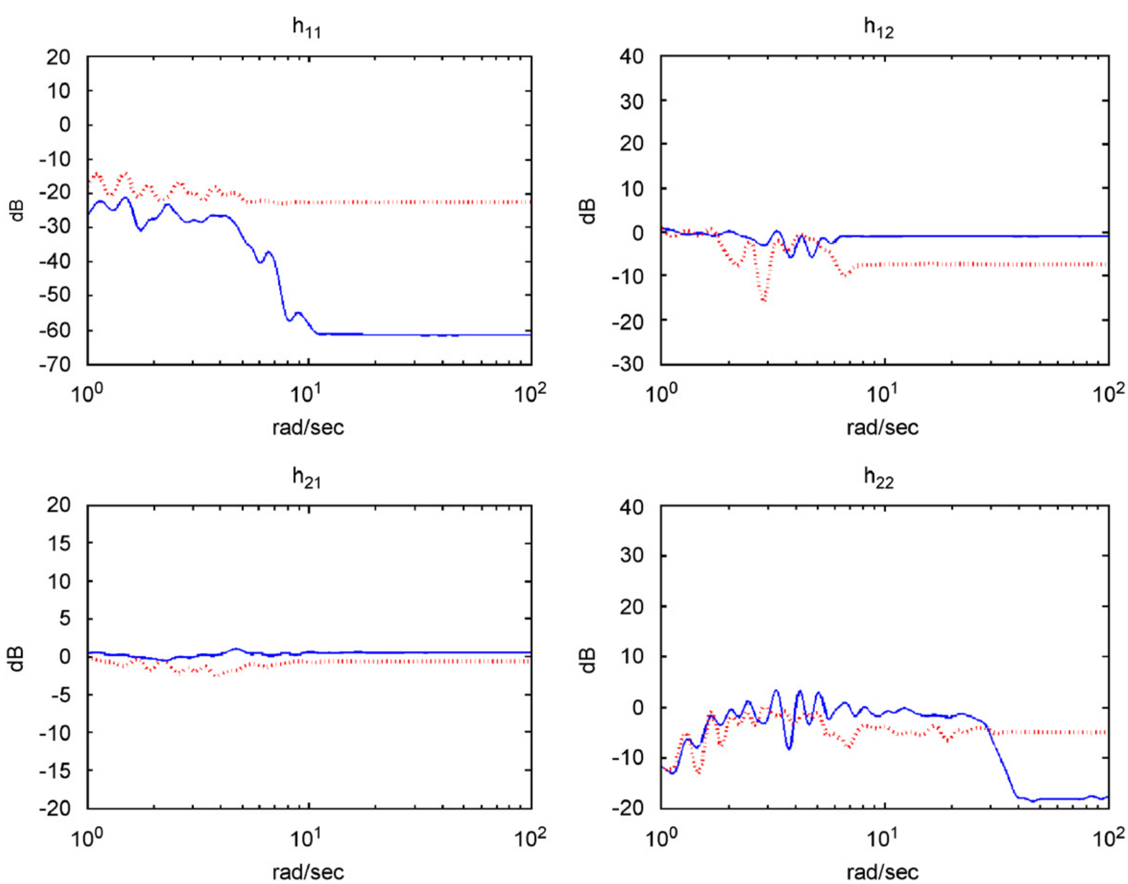

Fig. 13. Magnitudes of the hybrid parameters for the HPEB and HKFB teleoperation systems with one-way delay $T = 30\,\text{ms}$ (dashed: HPEB; solid: HKFB).

Fig. 11 shows the master and the slave position and torque tracking profiles for an HPEB teleoperation system implementation with $b = 1$, $T = 30\,\text{ms}$, $k_d = 3$, $k_p = 10$, and $f_{\text{cut}} = 5\,\text{Hz}$. This amount of time delay corresponds to the typical delay experienced in the terrestrial wired telecommunication link used for the telesurgery experiments reported in Rayman et al. (2005). Fig. 12 illustrates the same tracking profiles for an HKFB teleoperation system with similar parameters. As can be deduced from these figures, the position tracking performance for the two systems are close to each other. However, the HKFB teleoperation system displays a superior force tracking performance, which demonstrates a higher level of transparency. This deduction is in accordance with the simplified hybrid parameters in (38) and (39) and also the results presented in Sherman et al. (2000) and Aliaga et al. (2004), which have been derived for teleoperation systems without time delay.

To further investigate the relative transparency of these two systems, a second set of free-motion tests was performed, which in conjunction with the previous contact-mode tests, can be used to determine the hybrid parameters of the teleoperation system in the frequency domain. In this case, the problem is essentially one of closed-loop identifications. Closed-loop identification involves identifying a system that operates under output feedback and cannot be identified in open loop. In the context of bilateral teleoperation, the closed-loop system consists of the human operator, the teleoperation system, and the environment. The teleoperation system cannot be identified in open loop because in the absence of an environment (i.e., the slave in free space), two of the hybrid parameters (i.e., h_{12} and h_{22}) cannot be identified. Similarly, in the absence of a human in the loop, creating persistent-excitation force inputs is very difficult if not impossible.

In the following, the direct approach for closed-loop identification is utilized, in which the input and the output of the teleoperation system are used, ignoring any feedback or input, in order to obtain the hybrid model of the teleoperation system. In the free-motion tests, the master is moved back and forth by the user for about 100 s, while the slave's tip is in free space. Since $f_e = 0$, the frequency response $h_{11} = F_h/X_m$ and $h_{21} = -X_s/X_m$ can be found by applying spectral analysis (MATLAB function *spa*) on the free-motion test data (for the two-port hybrid model based on positions and forces). Then, by using the contact-mode test data, the other two hybrid parameters can be obtained as $h_{12} = F_h/F_e - h_{11}X_m/F_e$ and $h_{22} = -X_s/F_e - h_{21}X_m/F_e$. The magnitudes of the hybrid parameters of the HPEB and HKFB teleoperation systems for $T = 30\,\text{ms}$ are shown in Fig. 13. Due to the human operator's limited input bandwidth, these identified hybrid parameters can be considered valid up to frequency 100 rad/s. Fig. 13 is an indication of HKFB's superiority in terms of transparent performance considering the ideal transparency requirements outlined by (5). High values of h_{11} for HPEB are evidence of the fact that even when the slave is in free space, the user will feel some force as a result of any control inaccuracies (i.e., nonzero position errors), thus giving a "sticky" feel of free-motion movements. On the other hand, since HKFB uses f_e measurements, its input impedance in free-motion condition will be significantly lower making the feeling of free space much more realistic. The value of IAE for h_{11} with respect to the ideal case for the HPEB and HKFB configurations in Fig. 13, given in Table 2, further substantiate this conclusion. The better force tracking performance of HKFB in

Table 2
IAE values for deviations of the magnitudes of the H-parameters of HPEB and HKFB systems for one-way delays $T = 30$ and 300 ms

	$T = 30\,\text{ms}$		$T = 300\,\text{ms}$	
	HPEB	HKFB	HPEB	HKFB
h_{11}	8.8	1.9	8.3	1.8
h_{12}	46.3	13.1	200.9	21.0
h_{21}	10.1	4.6	12.1	3.5
h_{22}	59.1	63.0	157.0	63.9

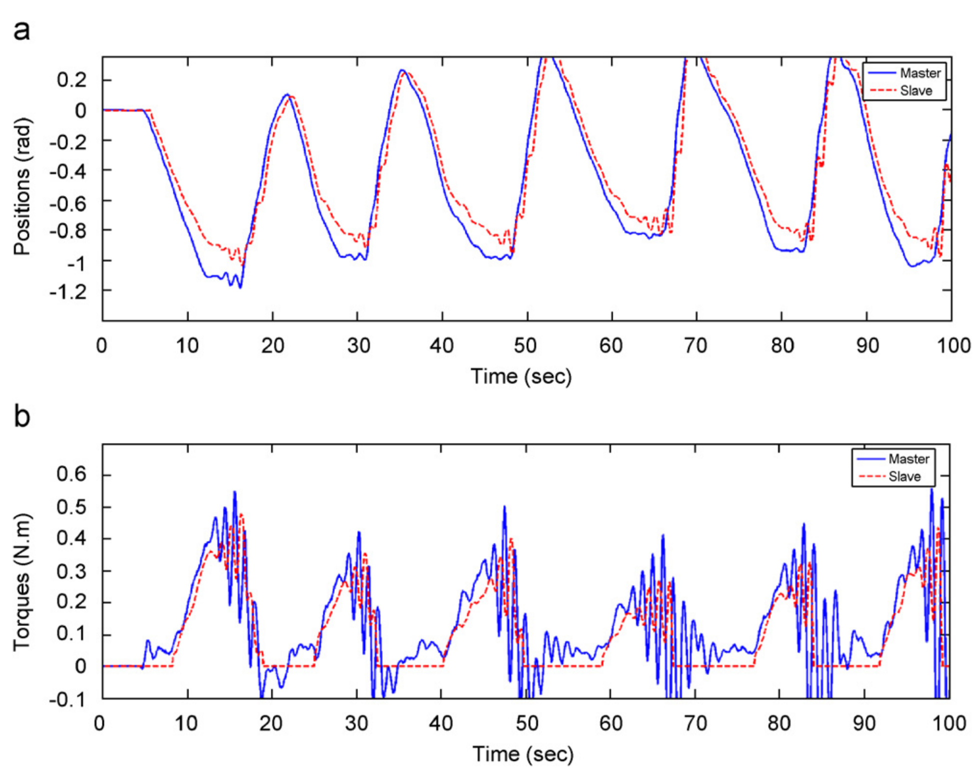

Fig. 14. (a) Position and (b) force tracking profiles for the HPEB teleoperation system with one-way delay $T = 300\,\text{ms}$.

Fig. 13, i.e., $h_{12} \approx 0$ dB, confirms the time-domain results observed in Figs. 11 and12 and also is in accordance with (38) and (39). With respect to h_{21}, both spectra seem to be close to 0 dB, which indicates both systems are capable of ensuring satisfactory position tracking. However, in this case IAE values in Table 2 are indicative of a better performance for HKFB configuration. It is

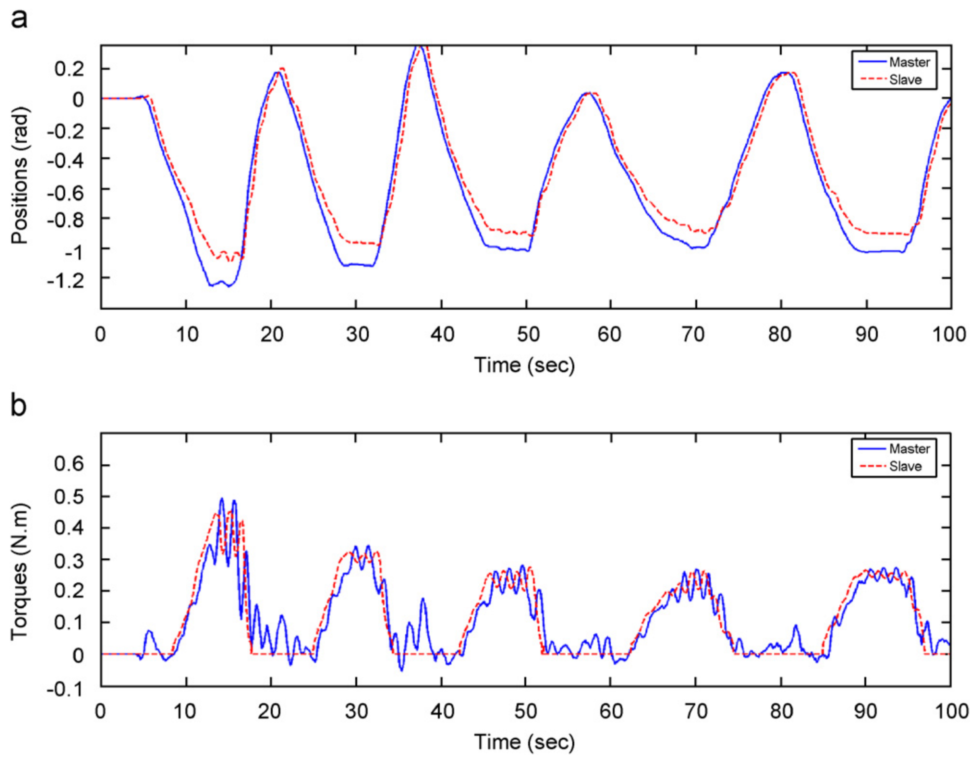

Fig. 15. (a) Position and (b) force tracking profiles for the HKFB teleoperation system with one-way delay $T = 300$ ms.

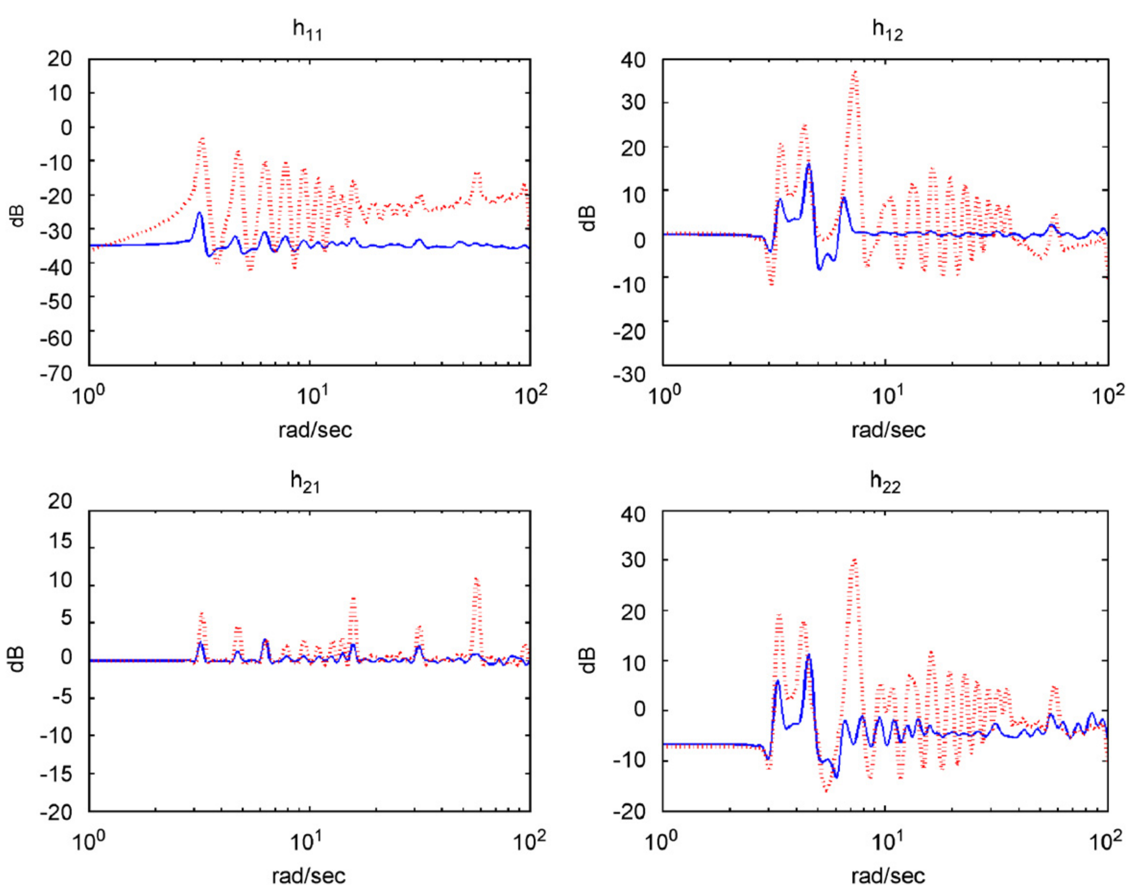

Fig. 16. Magnitudes of the hybrid parameters for HPEB and HKFB teleoperation systems with one-way delay $T = 300$ ms (dashed: HPEB; solid: HKFB).

worthwhile mentioning that because of the finite stiffness of the slave and also the backlash present in the slave's gearhead, the accuracy of h_{22} estimates is less than that of the rest of the hybrid parameters.

In order to study the transparency of the two teleoperation systems under larger time delays, the same experiments have been repeated for $T = 300$ ms. This is a typical upper bound for a single-hop satellite link's time delay (Rayman et al., 2005). Figs. 14 and 15 show the position and force tracking profiles for the HPEB and HKFB teleoperation systems, respectively. Fig. 16 shows the hybrid parameters for these two systems. As can be seen in Fig. 14, with HPEB configuration, there are vibrations in the master and slave positions and forces in the contact mode (with the magnitudes of vibrations increasing with time delay). While stability in the wave-based time delay compensation approach is guaranteed in theory regardless of the time delay, in practice and consistent with previous studies (Anderson & Spong, 1989; Niemeyer & Slotine, 1991; Ueda & Yoshikawa, 2004), such vibrations exist and may be due to implementation reasons such as discretization or limited controller bandwidth. As can be seen in Fig. 16, these vibrations affect the h_{12} parameter of the HPEB teleoperation system. However, as shown in the force profile of Fig. 15 and the h_{12} spectrum of Fig. 16, force tracking is much less subjected to unwanted vibrations in the case of HKFB configuration. The values of IAE for hybrid parameters of HPEB and HKFB configurations in Fig. 16 are given in Table 2. These results are indicative of the fact that transparency is improved by provision of slave force sensor data to the bilateral control algorithm.

6. Conclusion

In this paper, stability and transparency of different wave-based teleoperation systems have been comprehensively examined in the presence of communication time delays. Different wave transformation arrangements result in admittance-type and hybrid-type teleoperation architectures. Moreover, depending on the absence or presence of force sensing in the system, position error-based and kinesthetic force-based configurations are possible. Using an end-to-end model of the teleoperation system, it was analytically shown that stable admittance-type teleoperation systems can be implemented with or without direct force measurements. Additionally, based on a single-loop representation of the hybrid-type teleoperation system, stability of different configurations was investigated. Specifically, it was shown that stability can be maintained for such a teleoperation system when force measurements are used in the control configuration.

It was also demonstrated that in practice it is better to use a hybrid-type control architecture because simultaneous tuning of the two PD controllers in the admittance-type architecture can be problematic. Moreover, from a transparency point of view, it was shown that the use of force sensors provides better performance. In order to further substantiate the theoretical results, it was experimentally shown that using the measured force data can significantly improve transparency in the hybrid-type architecture. The experiments were conducted with 60 and 600 ms round-trip delays in a master/slave teleoperation system developed for robot-assisted telesurgery.

Future work on the topic of this paper will address the extension of the proposed schemes to a general multi degree-of-freedom master/slave teleoperation system and the problems with teleoperation stability and transparency that arise when a bilateral controller designed in the continuous-time domain is converted into the discrete-time domain for implementation as a digital controller.

Acknowledgments

This research was supported by the Natural Sciences and Engineering Research Council (NSERC) of Canada under Grants RGPIN-1345 and RGPIN-227612, the Ontario Research and Development Challenge Fund under Grant 00-May-0709 and infrastructure grants from the Canada Foundation for Innovation awarded to the London Health Sciences Centre (CSTAR) and the University of Western Ontario.

Appendix A. Stability regions in admittance-type teleoperation

(1) *Filtered APEB*

In order to derive stability condition (11) for the filtered APEB teleoperation system, condition (b) of Theorem 1 is applied to the singular values of the scattering matrix of filtered APEB teleoperation system while $s = \mathrm{j}\omega$. The result is the following condition set:

$$\begin{aligned}&k_d\omega^2L^2(b+k_d)+k_p^2L^2+2bk_d[1+\cos(\omega T)\\&\quad-L\sin(\omega T)]\geqslant 0\\&k_d\omega^2L^2(b+k_d)+k_p^2L^2+2bk_d[1-\cos(\omega T)\\&\quad+L\sin(\omega T)]\geqslant 0.\end{aligned} \tag{A.1}$$

These two conditions can be merged into the unified stability condition (11).

(2) *AKFB and filtered AKFB*

In the case of stability condition (15) for the AKFB teleoperation system, if the passivity condition is applied to the singular values in (14) while $s = \mathrm{j}\omega$ the resulting condition set is

$$\begin{aligned}&2bk_d\omega^2[b+\omega M\sin(\omega T)+b\cos(\omega T)]\geqslant 0\\&\quad-2bk_d\omega^2[-b+\omega M\sin(\omega T)+b\cos(\omega T)]\geqslant 0\end{aligned} \tag{A.2}$$

which can be combined as stability condition (15). For the filtered AKFB teleoperation system the resulting passivity condition set is

$$\begin{aligned}&-2\omega k_d(bL-M)\sin(\omega T)+2k_d(M\omega^2L+b)\cos(\omega T)\\&\quad+(k_db\omega^2L^2-Mk_p\omega^2L^2+k_d^2\omega^2L^2\\&\quad+L^2k_p^2+2bk_d)\geqslant 0\\&2\omega k_d(bL-M)\sin(\omega T)-2k_d(M\omega^2L+b)\cos(\omega T)\\&\quad+(k_db\omega^2L^2-Mk_p\omega^2L^2+k_d^2\omega^2L^2+L^2k_p^2+2bk_d)\geqslant 0\end{aligned} \tag{A.3}$$

which can be unified as the stability condition (16).

Appendix B. Master system modeling and identification

(1) *Dynamic modeling*

The 1-DOF dynamic model of the master in the twist direction

$$\tau_m = (m\ell^2 + I_{zz})\ddot{\theta}_m + mg\ell\sin(\theta_m + \alpha) \tag{B.1}$$

is needed for implementing the bilateral control laws discussed in the paper. Here, as shown in Fig. B-1, τ_m and θ_m are the joint torque and angular position at the motor output shaft, respectively. The center of mass m of the master is located at a distance ℓ and an angle α with respect to the master's axis of rotation. I_{zz} is the master's mass moment of inertia with respect to the axis of rotation.

Consider two rigid bodies that make contact through elastic bristles, the friction force/torque τ_{fric} between the two can be modeled based on their relative velocity $\dot{\theta}$ and the bristles's average deflection z as (de Wit, Olsson, Astrom, & Lischinsky, 1995):

$$\frac{\mathrm{d}z}{\mathrm{d}t} = \dot{\theta} - \sigma_0\frac{|\dot{\theta}|}{s(\dot{\theta})}z \tag{B.2}$$

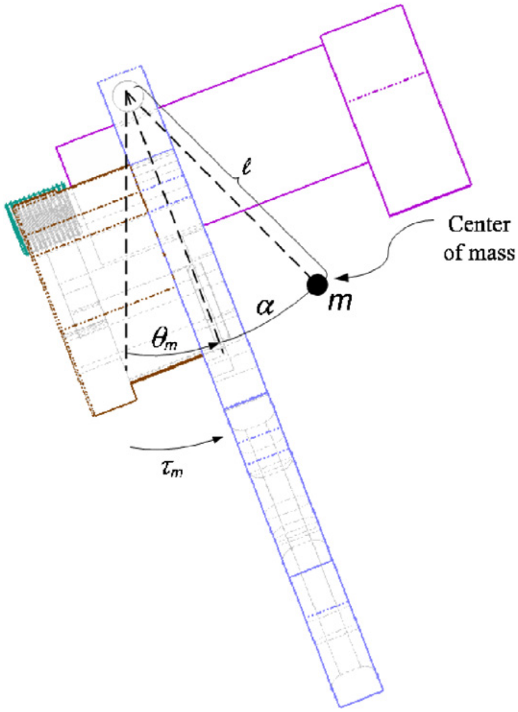

Fig. B-1. The master handle.

$$\tau_{\rm fric} = \sigma_0 z + \sigma_1 \frac{dz}{dt} + \sigma\dot{\theta} \tag{B.3}$$

where σ_0, σ_1 are stiffness and damping parameters for the friction dynamics, and the term $\sigma\dot{\theta}$ accounts for viscous friction. Using the Stribeck term $s(\dot{\theta}) = \tau_c(1 - e^{-a|\dot{\theta}|}) + \tau_s e^{-a|\dot{\theta}|}$ where τ_c and τ_s are Coulomb and stiction frictions respectively, friction can be written as

$$\tau_{\rm fric} = \sigma\dot{\theta} + \tau_c(1 - e^{-a|\dot{\theta}|})\mathrm{sgn}(\dot{\theta}) + \tau_s\, e^{-a|\dot{\theta}|}\mathrm{sgn}(\dot{\theta}) \tag{B.4}$$

For the master device, assuming asymmetry in Stribeck friction effects when the master moves in the positive and negative directions, the dynamics can be written as

$$\begin{aligned}\tau_m &= M_m\ddot{\theta}_m + G\sin(\theta_m + \alpha) + \sigma\dot{\theta}_m \\ &\quad + \tau_{c_1}(1 - e^{-a_1|\dot{\theta}_m|})u_{\dot{\theta}_m} + \tau_{s_1} e^{-a_1|\dot{\theta}_m|}u_{\dot{\theta}_m} \\ &\quad + \tau_{c_2}(1 - e^{-a_2|\dot{\theta}_m|})u_{-\dot{\theta}_m} + \tau_{s_2} e^{-a_2|\dot{\theta}_m|}u_{-\dot{\theta}_m}\end{aligned} \tag{B.5}$$

where τ_{c_i}, τ_{s_i} and a_i correspond to the positive direction ($\dot{\theta}_m > 0$) for $i = 1$ and to the negative direction ($\dot{\theta}_m < 0$) for $i = 2$, and $u(\cdot)$ is the unity step function.

(2) *Parametric identification*

The master dynamics (B.5) are unknown in terms of rigid-body parameters for inertia and gravity M_m, G, α and in friction parameters σ, τ_{c_1}, τ_{s_1}, a_1, τ_{c_2}, τ_{s_2}, and a_2. To identify these parameters, sinusoidal input torques with different amplitudes and frequencies were provided to the master. Using the obtained joint torque, position, velocity, and acceleration data, a nonlinear multivariable minimization procedure (Matlab function *fminimax*) was used to find the parameter estimates that best fit the dynamic model (B.5): $M_m = 5.97 \times 10^{-4}\,\mathrm{kg\,m^2}$, $G = 1.04 \times 10^{-1}\,\mathrm{N\,m}$, $\alpha = 9.3965^\circ$, $\sigma = 6.88 \times 10^{-4}\,\mathrm{N\,m\,s/rad}$, $\tau_{c_1} = 1.98 \times 10^{-2}\,\mathrm{N\,m}$, $\tau_{s_1} = 0\,\mathrm{N\,m}$, $a_1 = 55.2\,\mathrm{s/rad}$, $\tau_{c_2} = -1.62 \times 10^{-2}\,\mathrm{N\,m}$, $\tau_{s_2} = 0\,\mathrm{N\,m}$, and $a_2 = 42.1\,\mathrm{s/rad}$. The above identified parameters were used to compensate for the gravity and friction effects, thus simplifying the dynamic model of the master to $\tau_m = M_m\ddot{\theta}_m$.

References

Ahn, S. H., & Yoon, J. S. (2002). A bilateral control scheme for 2-dof telemanipulators with control input saturation. *Control Engineering Practice*, *10*(10), 1081–1090.

Aliaga, I., Rubio, A., & Sanchez, E. (2004). Experimental quantitative comparison of different control architectures for master–slave teleoperation. *IEEE Transactions on Control Systems Technology*, *12*(1), 2–11.

Anderson, R. J., & Spong, M. W. (1989). Bilateral control of teleoperators with time delay. *IEEE Transactions on Automatic Control*, *34*(5), 494–501.

Arcara, P., & Melchiorri, C. (2002). Control schemes for teleoperation with time delay: A comparative study. *Robotics and Autonomous Systems*, (38) 49–64.

Butner, S. E., & Ghodoussi, M. (2003). Transforming a surgical robot for human telesurgery. *IEEE Transactions on Robotics and Automation*, *19*(5), 818–824.

Colgate, J. E. (1993). Robust impedance shaping telemanipulation. *IEEE Transactions on Robotics and Automation*, *9*(4), 374–384.

de Wit, C. C., Olsson, H., Astrom, K. J., & Lischinsky, P. (1995). A new model for control systems with friction. *IEEE Transactions on Automatic Control*, *40*(3), 419–425.

Desoer, C. A., & Vidyasagar, M. (1975). *Feedback systems: Input– output properties*. New York: Academic Press.

Dodds, G., & Glover, N. (1995). Detailed modelling and estimation of practical robotic parameters for precision control. *Control Engineering Practice*, *3*(10), 1401–1408.

Guesalaga, A. (2004). Modelling end-of-roll dynamics in positioning servos. *Control Engineering Practice*, *12*(2), 217–224.

Guthart, G., & Salisbury, K., 2000. The intuitive telesurgery system: Overview and application, In *Proceedings of IEEE international conference on robotics and automation* (pp. 618–621).

Hannaford, B. (1989). A design framework for teleoperators with kinesthetic feedback. *IEEE Transactions on Robotics and Automation*, *5*(4), 426–434.

Hokayem, P. F., & Spong, M. W. (2006). Bilateral teleoperation: An historical survey. *Automatica*, *42*(12), 2035–2057.

Imaida, T., Yokokohji, Y., Doi, T., Oda, M., & Yoshikawa, T. (2004). Ground-space bilateral teleoperation of ETS-VII robot arm by direct bilateral coupling under 7-s time delay condition. *IEEE Transactions on Robotics and Automation*, *20*(3), 499–511.

Khalil, H. K. (2002). *Nonlinear systems* (3rd ed.). New Jersey: Prentice-Hall.

Lawrence, D. A. (1993). Stability and transparency in bilateral teleoperation. *IEEE Transactions on Robotics and Automation*, *9*(5), 624–637.

Lin, C. L., Chen, C. H., & Huang, H. C. (2008). Stabilizing control of networks with uncertain time varying communication delays. *Control Engineering Practice*, *16*(1), 56–66.

Mahvash, M., & Okamura, A., 2006. Friction compensation for a force-feedback telerobotic system. In *Proceedings of IEEE international conference on robotics and automation* (pp. 3268–3273), Orlando, FL.

Mascolo, S. (2006). Stabilizing control of networks with uncertain time varying communication delays. *Control Engineering Practice*, *14*(4), 425–435.

Niemeyer, G., & Slotine, J. J. E. (1991). Stable adaptive teleoperation. *IEEE Journal of Oceanic Engineering*, *16*(1), 152–162.

Preusche, C., Ortmaier, T., & Hirzinger, G. (2002). Teleoperation concepts in minimally invasive surgery. *Control Engineering Practice*, *10*(11), 1245–1250.

Rayman, R., Primak, S., Patel, S., Moallem, M., Morady, R., & Tavakoli, M. et al., 2005. Effects of latency on telesurgery: An experimental study. In *Proceedings of 8th international conference medical image computing and computer assisted intervention* (pp. 57–64), Palm Springs, CA.

Sheridan, T. B. (1995). Teleoperation, telerobotics, and telepresence: A progress report. *Control Engineering Practice*, *3*(2), 205–214.

Sherman, A., Cavusoglu, M.C., & Tendick, F., 2000. Comparison of teleoperator control architectures for palpation task. In *Proceedings of ASME dynamic systems and control division* (Vol. DSC 69-2), pp. 1261–1268.

Tanner, N. A., & Niemeyer, G. (2006). High-frequency acceleration feedback in wave variable telerobotics. *IEEE/ASME Transactions on Mechatronics*, *11*(2), 119–127.

Tavakoli, M., Patel, R.V., & Moallem, M. (2005). Haptic interaction in robot-assisted endoscopic surgery: A sensorized end-effector. *International Journal of Medical Robotics and Computer Assisted Surgery* (1), 53–63.

Tavakoli, M., Patel, R.V., & Moallem, M. (2006). A haptic interface for computer-integrated endoscopic surgery and training. *Virtual Reality* (9), 160–176.

Ueda, J., & Yoshikawa, T. (2004). Force-reflecting bilateral teleoperation with time delay by using signal filtering. *IEEE Transactions on Robotics and Automation*, *26*(3), 613–619.

Wagner, C.R., Stylopoulos, N., & Howe, R. (2002). The role of force feedback in surgery: Analysis of blunt dissection. In *The 10th symposium on haptic interfaces for virtual environment and teleoperator systems* (pp. 68–74), Orlando, FL (2002).

Yamamoto, S., & Kimura, H., 1995. On structured singular values of reciprocal matrices. In *Proceedings of the American control conference* (pp. 3358–3359).

Yokokohji, Y., & Yoshikawa, T. (1994). Bilateral control of master–slave manipulators for ideal kinesthetic coupling-formulation and experiment. *IEEE Transactions on Robotics and Automation*, *10*(5), 605–619.